Journal of Applied Mechanics and Technical Physics, Vol. 38, No. 5, 1997

THE PROBLEM OF A CONFINED EXPLOSION IN AN ELASTIC HALF-SPACE

A. I. Shakhov and N. I. Shishkin

UDC 550.348.425.4

The problem of propagation in ground of seismic waves generated by an underground explosion is usually formulated as the problem of propagation, in an elastic half-space, of waves generated by a localized source. This problem was examined in [1–3], where the motion of a free surface was studied. In this paper, we study displacements at internal points of the half-space and also residual displacements that occur therewith. The investigation of the motion of internal points of the medium is necessary for the analysis of elastic waves recorded upon underground explosions when the recording instruments are located inside the medium [4]. Buckling of the ground surface in an underground explosion is connected with residual displacements.

1. We examine the motion that occurs in an elastic half-space as a result of a confined explosion. The explosion occurs at depth $z = z_0$ under the free surface of the half-space related to the coordinate system $Or\theta z$ with the direction of the axes shown in Fig. 1. The center of the explosion is at the point $(r, z) = (0, z_0)$. Figure 1 also shows the edges of the waves that arise: the longitudinal wave P generated by the explosion, the longitudinal wave PP reflected from the free surface, and the reflected transverse wave PS.

The diverging spherical longitudinal wave generated by the explosion is described by the potential $\varphi^*(t, r, z)$ of the displacement field of a source that is equivalent to the explosion:

$$\varphi^*(t, r, z) = -\frac{\Phi(\infty)}{R} f\left[\frac{1}{t_0}\left(t - \frac{R}{c_P}\right)\right], \tag{1.1}$$

where $R = [r^2 + (z_0 - z)^2]^{1/2}$, $f(x) = 1 - (1 + x + x^2/2 + x^3/6 - Bx^4)\exp(-x)$, c_P is the propagation velocity of the longitudinal waves, and $\Phi(\infty)$, t_0, and B are the Haskell parameters that characterize the source [5].

The product $\Phi(\infty)f(x)$ is called the reduced potential [$\Phi(\infty)$ is the stationary value of the reduced potential, and $f(x)$ is the source function].

The parameter $\Phi(\infty)$, which has the dimension of volume, can be treated as the volume introduced into the elastic medium as a result of the explosion. It is proportional to the volume of the camouflet cavity and is related to its dimensions by the approximate relation [6] $\Phi(\infty) \approx r_c^3/3$, where r_c is the radius of the cavity.

The parameter t_0 — the characteristic time of wave radiation — is close to the ratio r_1/c_P, where r_1 is the radius of an elastic radiator that is equivalent to the explosion, or the Sharpe radius [7]. In turn, the value of r_1 is close to the radius of the rupture zone near the center of the explosion. According to the estimate of Rodionov [8], $r_1 = (E/3\sigma_*)^{1/3} r_c$, where E is Young's modulus and σ_* is the compression strength of the medium.

The dimension of the camouflet cavity can be calculated from empirical relations, for example, by the Heard formula [9]: $r_c = 16.3\, Q^{0.29}(E^{0.62}\rho_0^{-0.24}\mu^{-0.67}z_0^{-0.11})$ m [r_c and z_0 in meters, Q in ktons, μ (shear modulus) and E in megabars, and ρ_0 is the strength of the medium in grams per cubic centimeter].

The nondimensional parameter B is adjustable. It allows one to select the value of the reduced potential in accordance with the experiment. In this case, $0 \leqslant B \leqslant 0.5$.

The source function $f(x)$ satisfies the conditions $f(0) = f'(0) = f''(0) = f'''(0) = 0$, which ensure the continuity of the potential, displacement, velocity, and acceleration at the wave edge. In addition, $\lim\limits_{x\to\infty} f(x) = 1$.

FFNC–Institute of Technical Physics, Snezhinsk 456770. Translated from Prikladnaya Mekhanika i Tekhnicheskaya Fizika, Vol. 38, No. 5, pp. 3–15, September–October, 1997. Original article submitted July 10, 1995; revision submitted February 27, 1996.

0021-8944/97/3805-0655 $18.00

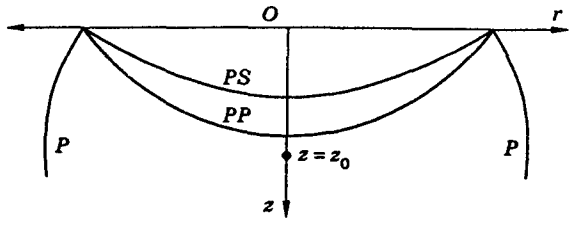

Fig. 1

In terms of the equations of the mechanics of continua, it suffices to require that the potential and displacement be continuous at the wave edge. The continuity of the velocity and acceleration are extra constraints that follow from experimental data on elastic waves generated by an underground explosion [5, 10].

Below, we shall use nondimensional variables and choose the characteristic time t_0 as the time scale, and $\lambda_0 = c_P t_0$ as the length scale. We shall retain the previous notation for all variables.

In the nondimensional variables, the source potential takes the form

$$\varphi^*(t,r,z) = -f(t-\rho_1)/\rho_1, \qquad \rho_1 = [r^2 + (z_0 - z)^2]^{1/2}. \tag{1.2}$$

The displacements produced by the source (1.2) in an infinite medium are written as

$$\mathbf{u}^*(t,r,z) = u_r^*(t,r,z)\mathbf{r}_1 + u_z^*(t,r,z)\mathbf{z}_1. \tag{1.3}$$

Here

$$u_r^* = \frac{\partial \varphi^*}{\partial r} = \frac{r}{\rho_1}\left[\frac{f'(t-\rho_1)}{\rho_1} + \frac{f(t-\rho_1)}{\rho_1^2}\right]; \quad u_z^* = \frac{\partial \varphi^*}{\partial z} = -\frac{z_1}{\rho_1}\left[\frac{f'(t-\rho_1)}{\rho_1} + \frac{f(t-\rho_1)}{\rho_1^2}\right],$$

where $z_1 = z_0 - z$, and $\mathbf{r}_1$ and $\mathbf{z}_1$ are the unit vectors of the coordinate axes. In this case, the dimensional displacements are

$$\frac{\Phi(\infty)}{(c_P t_0)^2} u_r^* \quad \text{and} \quad \frac{\Phi(\infty)}{(c_P t_0)^2} u_z^*.$$

2. The displacements in the half-space are written as the sum

$$\mathbf{u}^*(t,r,z) + \mathbf{u}(t,r,z), \tag{2.1}$$

where $\mathbf{u}(t,r,z)$ are the displacements caused by the reflection of the wave generated by the source from the free surface. The integral representation of the displacement field $\mathbf{u} = u_r\mathbf{r}_1 + u_z\mathbf{z}_1$ is obtained in [2]. It is of the form

$$u_r(t,r,z) = -\gamma \int_0^\infty k^2 J_1(kr)\left[\frac{1}{2\pi i}\int_l \frac{\Delta_1}{\alpha_1 \Delta}\exp(-kz_2\alpha_1 + k\gamma t\zeta)F(k\gamma\zeta)\,d\zeta\right]dk$$

$$+\gamma \int_0^\infty k^2 J_1(kr)\left[\frac{1}{2\pi i}\int_l \frac{\beta_1\Delta_2}{\Delta}\exp(-kz_0\alpha_1 - kz\beta_1 + k\gamma t\zeta)F(k\gamma\zeta)\,d\zeta\right]dk, \tag{2.2}$$

$$u_z(t,r,z) = -\gamma \int_0^\infty k^2 J_0(kr)\left[\frac{1}{2\pi i}\int_l \frac{\Delta_1}{\Delta}\exp(-kz_2\alpha_1 + k\gamma t\zeta)F(k\gamma\zeta)\,d\zeta\right]dk$$

$$+\gamma \int_0^\infty k^2 J_0(kr)\left[\frac{1}{2\pi i}\int_l \frac{\Delta_2}{\Delta}\exp(-kz_0\alpha_1 - kz\beta_1 + k\gamma t\zeta)F(k\gamma\zeta)\,d\zeta\right]dk,$$

where $\Delta = \delta_1^2 - 4\alpha_1\beta_1$, $\Delta_1 = \delta_1^2 + 4\alpha_1\beta_1$, $\Delta_2 = 4\delta_1$, $\delta_1 = 2 + \zeta^2$, $\alpha_1 = \sqrt{1+\gamma^2\zeta^2}$, $\beta_1 = \sqrt{1+\zeta^2}$, $z_2 = z_0 + z$, $\gamma = c_S/c_P$, $\operatorname{Re}\alpha_1 = \operatorname{Re}\beta_1 = 0$ for $\zeta > 0$, l is the contour of integration in the formula of the inverse

Laplace transform [11], $F(\gamma k\zeta)$ is the Laplace transform of the function $f(t)$, and $J_0(kr)$ and $J_1(kr)$ are Bessel functions.

In contrast to [2], in formulas (2.2), the transform of the source function $F(\gamma k\zeta)$ is introduced explicitly and misprints are corrected.

As the fundamental solution we use the solution that corresponds to

$$F(\gamma k\zeta) = (\gamma k\zeta)^{-2} \doteq t, \tag{2.3}$$

where symbol $\doteq$ denote the Laplace transform.

The terms of the fundamental solution due to the longitudinal and transverse potentials of the displacement field are denoted by $\mathbf{U}^P(t,r,z)$ and $\mathbf{U}^S(t,r,z)$, respectively. Then, the general solution that corresponds to the source function $f(t)$ is represented as the convolution of the fundamental solution with the second derivative of the function source:

$$\mathbf{u}(t,r,z) = \mathbf{u}^* + \int_0^{t-t_P} \mathbf{U}^P(t-\tau,r,z)f''(\tau)\,d\tau + \int_0^{t-t_S} \mathbf{U}^S(t-\tau,r,z)f''(\tau)\,d\tau. \tag{2.4}$$

Here $\mathbf{u}^* = \mathbf{u}^*(t,r,z)$ is the displacement field produced by the source (1.1) in an infinite elastic medium, $t_P = (r^2+z_2^2)^{1/2}$ is the time of arrival of the reflected longitudinal wave at the observation point, and t_S is a similar moment for the transverse wave. In this case,

$$t_S = \sqrt{z_0^2+C^2} + \frac{1}{\gamma}\sqrt{(r-C)^2+z^2},$$

where C is a positive root of the equation $(r-C)\sqrt{z^2+C^2} - \gamma C\sqrt{(r-C)^2+z^2} = 0$.

The approximate values of the parameter C obtained by the iterative method are of the form

$$C \approx C_n = r(1-\varepsilon_n) \qquad (n = 0,\ 1,\ 2,\ \ldots),$$

$$\varepsilon_n = \gamma(1-\varepsilon_{n-1})\left[\frac{\varepsilon_{n-1}^2 r^2 + z^2}{(1-\varepsilon_{n-1})^2 r^2 + z_0^2}\right]^{1/2}, \quad \varepsilon_0 = 0, \quad \varepsilon_1 = \gamma z/\sqrt{r^2+z_0^2}.$$

3. An explicit expression for the fundamental solution can be obtained in the same manner as was done in [1, 2]. That is, first one should deform the contour l in (2.2) so that it embraces the cuts of the ζ plane drawn from the branching points. The branching points are the zero of the radicals α_1 and β_1, and the cuts are drawn along the imaginary axis to infinity. Then, taking into account residues at the poles of the integrands for $\zeta = 0$ and $\zeta = \pm i\vartheta$, where ϑ is a root of the Rayleigh equation $2-\vartheta^2 = 4\sqrt{1-\gamma^2\vartheta^2}\sqrt{1-\vartheta^2}$, one should take Fourier–Bessel integrals of the real variable k.

As a result we obtain the following expressions for the fundamental solution:

$$\begin{aligned} U_r^P &= U_{r0}^P + U_{rR}^P + U_{r\lambda}^P, \qquad U_z^P = U_{z0}^P + U_{zR}^P + U_{z\lambda}^P, \\ U_r^S &= U_{r0}^S + U_{rR}^S + U_{r\lambda}^S, \qquad U_z^S = U_{z0}^S + U_{zR}^S + U_{z\lambda}^S. \end{aligned} \tag{3.1}$$

In formulas (3.10), the terms with the subscript 0 are written as

$$\begin{aligned} U_{r0}^P &= \frac{2\gamma^2}{1-\gamma^2}\left(\frac{1}{1-\gamma^2} + \frac{3z_2^2}{\rho_2^2} - \frac{4z_2^2-r^2}{\rho_2^4}t^2\right)\frac{r}{\rho_2^3}\,t\varepsilon(t-t_P), \\ U_{r0}^S &= \frac{2\gamma^2}{1-\gamma^2}\left[\frac{1-2\gamma^2-\gamma^4}{2\gamma^2(1-\gamma^2)} - 3\left(z_0+\frac{z}{\gamma^2}\right)\frac{z_2}{\rho_2^2} + \frac{4z_2^2-r^2}{\rho_2^4}t^2\right]\frac{r}{\rho_2^3}\,t\varepsilon(t-t_S), \\ U_{z0}^P &= \frac{2\gamma^2}{1-\gamma^2}\left(\frac{\gamma^2}{1-\gamma^2} + \frac{2z_2^2-r^2}{\rho_2^2} - \frac{2z_2^2-3r^2}{\rho_2^4}t^2\right)\frac{z_2}{\rho_2^3}\,t\varepsilon(t-t_P), \\ U_{z0}^S &= \frac{2\gamma^2}{1-\gamma^2}\left[-\frac{1+\gamma^4}{2\gamma^2(1-\gamma^2)} - \frac{1}{z_2}\left(z_0+\frac{z}{\gamma^2}\right)\frac{2z_2^2-r^2}{\rho_2^2} + \frac{2z_2^2-3r^2}{\rho_2^4}t^2\right]\frac{z_2}{\rho_2^3}\,t\varepsilon(t-t_S), \end{aligned} \tag{3.2}$$

where $\varepsilon(t)$ is the Heaviside function. They are obtained by finding the residue at the pole of the fourth order, which has the integrands in the contour integrals (2.2). These are low-frequency or quasi-static components of displacements.

The terms with the subscript R describe the Rayleigh wave:

$$U_{rR}^P = \frac{4ab^2}{\gamma\vartheta^3\theta} S_1(r, az_2, \gamma\vartheta t)\varepsilon(t - t_P), \quad U_{rR}^S = -\frac{2ab^2d}{\gamma\vartheta^3\theta} S_1(r, az_0 + bz, \gamma\vartheta t)\varepsilon(t - t_S),$$
$$U_{zR}^P = \frac{4a^2b^2}{\gamma\vartheta^3\theta} S_0(r, az_2, \gamma\vartheta t)\varepsilon(t - t_P), \quad U_{zR}^S = -\frac{2abd}{\gamma\vartheta^3\theta} S_0(r, az_0 + bz, \gamma\vartheta t)\varepsilon(t - t_S). \tag{3.3}$$

Here $a = \sqrt{1 - \gamma^2\vartheta^2}$, $b = \sqrt{1 - \vartheta^2}$, $d = 2 - \vartheta^2$; $\theta = abd - (a^2 + \gamma^2 b^2)$, and $\vartheta = \vartheta(\gamma)$ is a root of the Rayleigh equation $d^2 - 4ab = 0$ that is a function of the parameter γ. The functions of three arguments S_1 and S_0 are of the form

$$S_1(r, p, q) \equiv \int_0^\infty J_1(kr)\, \exp(-kp)\, \sin(kq)\, dk = \frac{qA - pB}{rR},$$

$$S_0(r, p, q) \equiv \int_0^\infty J_0(kr)\, \exp(-kp)\, \sin(kq)\, dk = \frac{B}{R},$$

where

$$A = \left(\frac{R + X}{2}\right)^{1/2}; \quad B = \left(\frac{R - X}{2}\right)^{1/2}; \quad R = (X^2 + Y^2)^{1/2}; \quad X = r^2 + p^2 - q^2; \quad Y = 2pq.$$

The terms with the subscript λ (the high-frequency components of the displacement field) are expressed by the following formulas:

$$U_{r\lambda}^P = -\frac{\varepsilon(t - t_P)}{\gamma\pi} \int_1^{1/\gamma} \frac{16\,\delta^2\beta}{\lambda^2(\delta^4 + 16\,\alpha^2\beta^2)} S_1(r, \alpha z_2, \gamma t\lambda)\, d\lambda,$$

$$U_{r\lambda}^S = \frac{\varepsilon(t - t_S)}{\gamma\pi} \int_1^{1/\gamma} \frac{4\,\beta\delta G_r(r, z, \lambda)}{\lambda^2(\delta^4 + 16\,\alpha^2\beta^2)}\, d\lambda,$$

$$G_r(r, z, \lambda) = [S_1(r, \alpha z_0, \gamma t\lambda + \beta z) + S_1(r, \alpha z_0, \gamma t\lambda - \beta z)]\delta^2 - 4\alpha\beta[C_1(r, \alpha z_0, \gamma t\lambda + \beta z) - C_1(r, \alpha z_0, \gamma t\lambda - \beta z)],$$

$$U_{z\lambda}^P = \frac{-\varepsilon(t - t_P)}{\gamma\pi} \int_1^{1/\gamma} \frac{16\,\alpha\beta\delta^2}{\lambda^2(\delta^4 + 16\,\alpha^2\beta^2)} S_0(r, \alpha z_2, \gamma t\lambda)\, d\lambda,$$

$$U_{z\lambda}^S = \frac{\varepsilon(t - t_S)}{\gamma\pi} \int_1^{1/\gamma} \frac{4\,\delta G_S(r, z, \lambda)}{\lambda^2(\delta^4 + 16\,\alpha^2\beta^2)}\, d\lambda, \tag{3.4}$$

$$G_S(r, z, \lambda) = 4\alpha\beta[S_0(r, \alpha z_0, \gamma t\lambda + \beta z) + S_0(r, \alpha z_0, \gamma t\lambda - \beta z)] + \delta^2[C_0(r, \alpha z_0, \gamma t\lambda + \beta z) - C_0(r, \alpha z_0, \gamma t\lambda - \beta z)],$$

$$C_1(r, p, q) \equiv \int_0^\infty J_1(kr)\, \exp(-kp)\, \cos(kq)\, dk = \frac{1}{r}\left(1 - \frac{pA + qB}{R}\right),$$

$$C_0(r, p, q) \equiv \int_0^\infty J_0(kr)\, \exp(-kp)\, \cos(kq)\, dk = \frac{A}{R}.$$

Here $\alpha = \sqrt{1 - \gamma^2\lambda^2}$, $\beta = \sqrt{\lambda^2 - 1}$, and $\delta = 2 - \lambda^2$. The velocities and accelerations are given by the derivatives of the displacements with respect to time: $\mathbf{v} = \partial\mathbf{u}/\partial t$ and $\mathbf{w} = \partial^2\mathbf{u}/\partial t^2$.

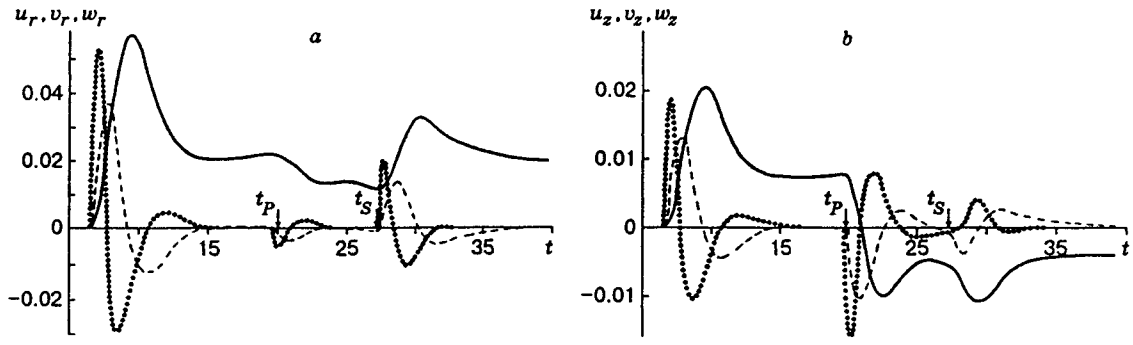

Fig. 2

The formulas for the displacements of the free surface follow from (1.2) and (3.1)–(3.4) for $z = 0$. The fundamental solution in this case (it was obtained in [2]) is written as

$$U_r(t,r,0) = \varepsilon(t-\rho)\left[\frac{2rt}{(1-\gamma^2)\rho^3} + \frac{2ab^2}{\gamma\vartheta\theta} S_1(r, az_0, \gamma\vartheta t) - \frac{1}{\gamma\pi}\int_1^{1/\gamma} \frac{8\beta\delta^2}{\Delta} S_1(r, \lambda z_0, \gamma\lambda t)\, d\lambda\right],$$
$$U_z(t,r,0) = \varepsilon(t-\rho)\left[-\frac{2z_0 t}{(1-\gamma^2)\rho^3} - \frac{abd}{\gamma\vartheta\theta} S_0(r, az_0, \gamma\vartheta t) - \frac{1}{\gamma\pi}\int_1^{1/\gamma} \frac{16\alpha\beta\delta}{\Delta} S_0(r, \lambda z_0, \gamma\lambda t)\, d\lambda\right], \tag{3.5}$$

where $\Delta = \delta^4 + 16\alpha^2\beta^2$.

The general solution is expressed by the formulas

$$u_r(t,r,0) = \int_0^{t-\rho} U_r(t-\tau, r, 0) f''(\tau)\, d\tau, \quad u_z(t,r,0) = \int_0^{t-\rho} U_z(t-\tau, r, 0) f''(\tau)\, d\tau. \tag{3.6}$$

The quasi-static terms of displacements can be obtained in explicit form. Thus, substituting the first terms of formulas (3.5) into (3.6), we obtain

$$U_{r0} = \frac{2r}{(1-\gamma^2)\rho^3}\int_0^{t-\rho}(t-\tau) f''(\tau)\, d\tau = \frac{2r}{(1-\gamma^2)\rho}\left[\frac{f'(t-\rho)}{\rho} + \frac{f(t-\rho)}{\rho^2}\right],$$
$$U_{z0} = -\frac{2z_0}{(1-\gamma^2)\rho}\left[\frac{f'(t-\rho)}{\rho} + \frac{f(t-\rho)}{\rho^2}\right], \qquad \rho = (z^2 + z_0^2)^{1/2}. \tag{3.7}$$

Similar formulas for the quasi-static terms of the displacement field can be obtained in the general case for $z \neq 0$.

4. The vibration characteristics at internal points of the elastic half-space are given in Fig. 2, which shows the horizontal (a) and vertical (b) components of displacements, velocities, and accelerations (solid, dashed, and dotted curves, respectively) versus time at a point with coordinates $r = 6.218$ and $z = 10.43$ for a source depth of $z_0 = 8.25$. These coordinates correspond to one point of observation of the "Salmon" nuclear explosion performed in the United States in 1964. Data on this explosion test are given in [12–16]. The "Salmon" explosion with an energy field of 5.3 ktons $= 2.2 \cdot 10^{13}$ J was carried out in a mass of stone salt at a depth of 827.8 m.

The physicomechanical parameters of stone salt are as follows: density $\rho_0 = 2160$ kg/m^3, velocity of longitudinal elastic waves $c_P = 4670$ m/sec, and Poisson ratio $\nu = 0.24$. The dimensional coordinates of the observation point considered are as follows: tilted distance from the center of explosion $\rho_1 = 659.6$ m, horizontal distance $r = 621.8$ m, and vertical coordinate $z = 1043$ m.

The Haskell potential parameters that we calculated from the oscillograms in [4] of ground displacement

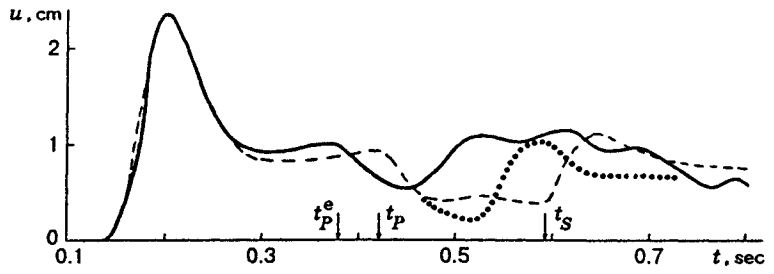

Fig. 3

in the "Salmon" test are as follows:

$$\Phi(\infty) = 3770 \text{ m}^3, \qquad t_0 = 0.0214 \text{ sec}, \qquad B = 0.060. \tag{4.1}$$

They were chosen from the condition of better fit of the calculated radial displacements to the experimental displacement curves in the initial portions of the oscillograms in [4] that correspond to the region of the direct wave.

The radial displacement was calculated from the formula

$$u_{\rho_1} = \mathbf{u} \cdot \mathbf{e} = (u_r \mathbf{r}_1 + u_r \mathbf{z}_1) \cdot \left(\frac{r}{\rho_1} \mathbf{r}_1 + \frac{z - z_0}{\rho_1} \mathbf{z}_1 \right) = \frac{r u_r}{\rho_1} + \frac{(z - z_0) u_z}{\rho_1},$$

where $\mathbf{e}$ is the unit vector in the direction from the center of explosion to the point of observation.

It can be seen from Fig. 2 that the motion is represented as a sequence of three pulses that correspond to the vibrations in the direct wave (from the moment of arrival to the moment t_P), vibrations in the reflected longitudinal wave (from t_P to t_S), and vibrations in the reflected transverse wave (after the moment t_S). In this case, the motion in the longitudinal wave reflected from the free surface is reverse, and the motion in the reflected transverse wave is similar to the motion in the direct wave. The fourth pulse, due to the Rayleigh wave at the point considered, has a small amplitude and cannot be seen against the background of the general motion.

Figure 3 shows oscillograms of the radial displacement at the same point as in Fig. 2. The solid curve refers to the experiment, and the dashed curve refers to the calculation. As can be seen from Fig. 3, the shape of the displacement curve in the direct wave (from the moment of arrival to the moment $t = t_P$) practically coincides with the shape of the reduced potential, i.e., the source function $f(t)$. This might be expected, because, in this case, the distance $\rho_1 = 6.6$ is relatively large, and, in formula (1.3), the second term, which is proportional to the value of the source function, dominates.

Further, in the time interval from 0.38 to 0.52 sec, a pulse appears which is apparently due to the longitudinal wave reflected from the free surface. Its location correlates with the position of the reflected wave in the calculated curve. But the shapes of the calculated and experimental pulses are different.

In the calculation, the reflected pulse has three phases: the motion to the center of explosion, which begins after the arrival of the longitudinal wave at the moment $t = t_P$ (first phase), the state of rest after the maximal displacement to the center of explosion up to the moment $t = t_S$ — the onset of the transverse wave (second phase), and the motion from the center of explosion at $t > t_S$ (third phase).

In the experiments, the reflected pulse consists of two phases: the first and the third, which form a single dome-shaped pulse. The second phase is not observed.

Increasing the calculated velocity of transverse waves c_S, one can find a value of the velocity such that the reflected pulse becomes similar to the experimental pulse. This is the case for $c_S = 3240$ m/sec, which corresponds to $\nu \approx 0.038$ ($\gamma = 0.695$). The calculated displacement for $\nu = 0.24$ ($\gamma = 0.595$) is shown in Fig. 3 by the dashed curve, and the displacement for $\nu = 0.038$ ($\gamma = 0.695$) is shown by the dotted curve . Thus, the best agreement between the calculation and the experiment is achieved for the Poisson ratio much smaller than 0.24 (this value is obtained by laboratory measurements).

A similar result — the best agreement between the calculation and the experiment for $\nu \approx 0.03$–0.04 — takes place for all the oscillograms in [4] in which the pulse that corresponds to the wave reflected from the free surface can be identified. These oscillograms were obtained at distances of 318.2, 321.0, 401.7, and 659.6 m from the center of explosion. In the other oscillograms given in [4], the wave pulses reflected from the free surface are concealed by the noise due to the inhomogeneity of the medium.

The small value of the Poisson ratio indicates that the stretching or shortening of the element of the medium proceeds without considerable shortening of its transverse dimensions. Thus, it can be seen that stone salt in the seismic waves generated by the "Salmon" explosion was deformed as a porous medium. According to the data of [14], the volume porosity of stone salt determined before the explosion was 3.14%.

One more difference between the calculation and the experiment should be noted in Fig. 3. For the velocity of the transverse waves used in the calculations, $c_P = 4670$ m/sec [4], the reflected longitudinal wave appears 0.05 sec later than in the experiment (in the calculation, $t_P = 0.43$ sec, and, in the experiment, $t_P^e = 0.385$ sec). Coincidence of the times of arrival of the reflected waves occurs when the calculated velocity of longitudinal waves $c_P = 5110$ m/sec. For stone salt with the physical characteristics given in [14], the longitudinal waves cannot have such a high velocity. It is possible that, in the experiment, the wave that was recorded was reflected from the lower boundary of the loose sediment layer and not from the Earth's surface. The thickness of this layer is about 70 m (Fig. 1 in [14]).

Figure 4 gives calculated results for the displacements, velocities, and accelerations at distances $r = 0$, 2, 10, and 30 from the zero point at a depth of the source $z_0 = 1$ (the solid curves refer to the displacements, the dashed curves refer to the velocity, the dotted curves refer to accelerations, and the letter R denotes vibrations in the Rayleigh wave). These oscillograms give an insight into the character of motion of the free surface of the half-space for the source parameters (4.1). The results of calculation of the motion of the free surface obtained by formulas (3.5) and (3.6) agree with the results calculated from the formulas of [3], where a different representation of the fundamental solution is used.

5. The Haskell source (1.1) is remarkable for the fact that it models not only the elastic wave generated by an underground explosion, but also the residual displacements and stresses that occur in the ground.

The displacements produced by the source in an infinite elastic medium are of the form

$$u_*(R,t) = \frac{\partial \varphi_*}{\partial R} = \Phi(\infty)\left[\frac{f(x)}{R^2} + c_P t_0 \frac{f'(x)}{R}\right], \tag{5.1}$$

where $x = (t - R/c_P)/t_0$, and R is the distance from the center of the explosion. In (5.1) and below we use dimensional variables.

Passing to the limit $t \to \infty$ in (5.1) and taking into account that $f(\infty) = 1$ and $f'(\infty) = 0$, for residual displacements we have [5]

$$u_*^\infty = \lim_{t\to\infty} u_*(R,t) = \Phi(\infty)/R^2. \tag{5.2}$$

For the residual stresses we obtain the formulas

$$\sigma_r^\infty = 4\gamma^2 \rho c_P^2 \frac{\Phi(\infty)}{R^3}, \qquad \sigma_\vartheta^\infty = \sigma_\varphi^\infty = 2\gamma^2 \rho c_P^2 \frac{\Phi(\infty)}{R^3}. \tag{5.3}$$

The physical cause of the occurrence of static fields of the form of (5.2) and (5.3) is the formation of a camouflet cavity surrounded by zones of fragmentation and radial cracks at the center of explosion [8]. The cavity and rupture zones that arise prevent the unloading of the state (5.3). The rupture zone around the cavity is a spherical shell, which has a load-carrying capacity. The carrying capacity of this zone is sufficient to preserve residual displacements and stresses for some time, which is much larger than the characteristic time t_0.

The parameter $\Phi(\infty)$ can be determined directly from the oscillogram of displacement of any point of the medium in the region of the direct wave. From formula (5.2) we can find the residual displacement u_*^∞ and then calculate the volume displaced into the elastic zone:

$$V_\infty = 4\pi R^2 u_*^\infty(R) = 4\pi R^2 \Phi(\infty)/R^2 = 4\pi\Phi(\infty). \tag{5.4}$$

If, before the explosion, the medium did not have porosity, the volume V_∞ is the sum of the volume of

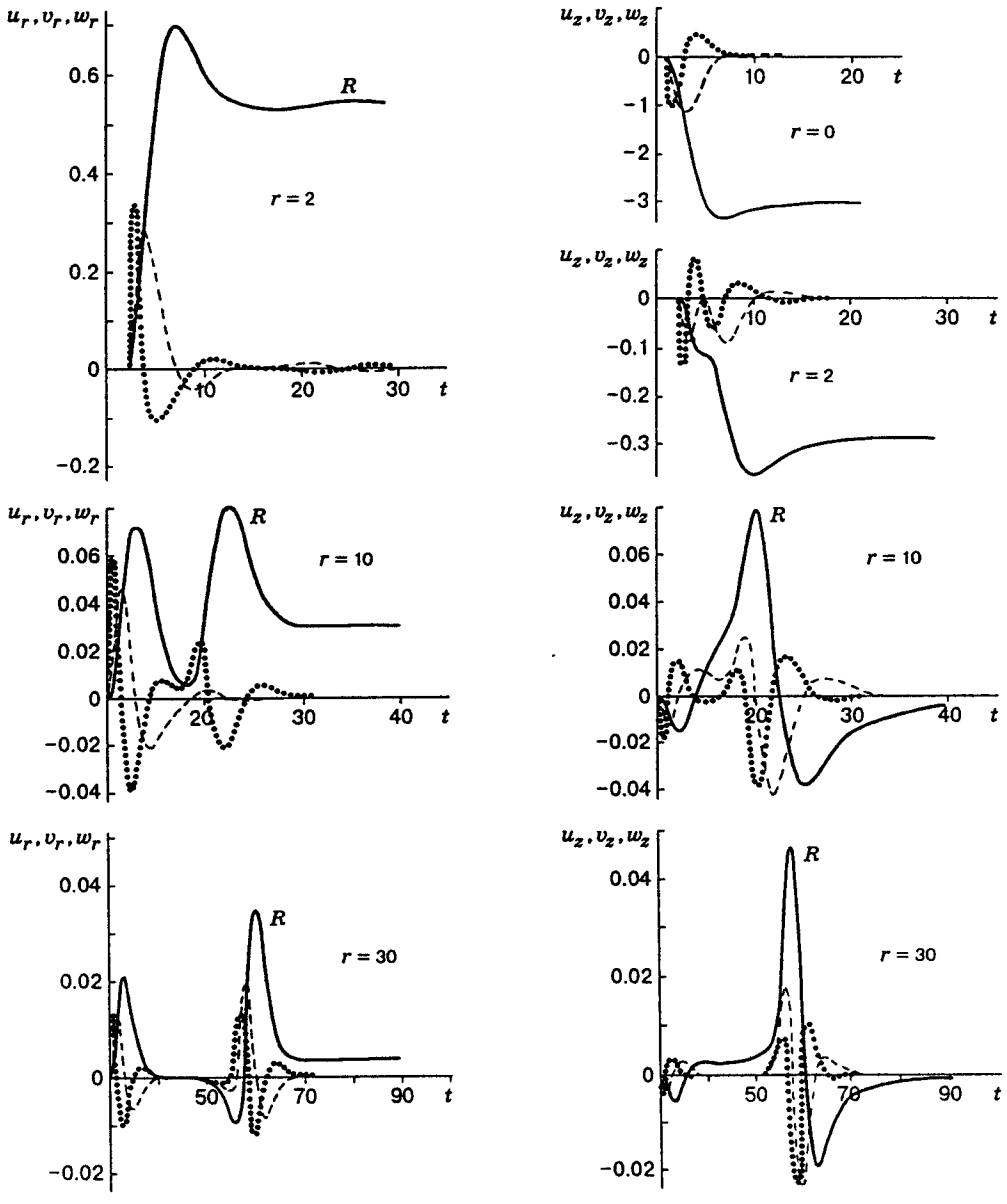

Fig. 4

the cavity and the volume of the voids produced in the ground by the explosion:

$$V_\infty = V_c + V_* = \frac{4}{3}\pi r_c^3 + V_*. \tag{5.5}$$

Here V_c and r_c are the volume and radius of the cavity, and V_* is the volume of the voids.

From (5.4) and (5.5) we obtain the following expression for the volume of the voids:

$$V_* = 4\pi\Phi(\infty) - \frac{4}{3}\pi r_c^3. \tag{5.6}$$

For the "Salmon" explosion, $\Phi(\infty) = 3770$ m^3 [see (4.1)], and the radius of the cavity $r_c = 16.7$ m [16]. It follows from (5.4) and (5.6) that the displaced volume is $V_\infty = 47{,}400$ m^3, the volume of the cavity $V_c = 19{,}400$ m^3, and the volume of the voids $V_* = 28{,}000$ m^3.

Radial cracks, according to the data of [16], were observed at distances of 90 to 120 m from the center of explosion. Then, assuming the radius of the rupture zone to be equal to the half-sum of these values ($r_r = 105$ m), we obtain an estimate for the porosity of the stone salt in the "Salmon" explosion:

$$\eta = \frac{V_*}{V_r - V_c} = \frac{V_\infty - V_c}{V_r - V_c} = \frac{4\pi\Phi(\infty) - (4/3)\pi r_c^3}{(4/3)\pi(r_r^3 - r_c^3)} \simeq 0.58 \cdot 10^{-2} \approx 0.6\%.$$

As can be seen, even insignificant loosening of the ground in the explosion leads to the fact that most of the displaced volume is formed by rupture zones rather than by the cavity.

In connection with the above estimates, we should note the following. In [16], the dimension of the cavity formed in the "Salmon" explosion, $r = 16.7$ m, was obtained by measuring the cavity 45 months after the explosion. In the estimation in this section, we use, strictly speaking, the radius of the cavity that occurs "just after the explosion." During the several months that passed after the explosion, the stress state (5.3) could have been partially unloaded, and, as a result, the volume of the initial cavity could have decreased.

6. In the case of the half-space bounded by the free surface, the residual displacements can also be obtained from formulas (2.4), (3.1)–(3.4) by passage to the limit $t \to \infty$. With this passage, only the terms obtained from the quasi-static terms of the displacement field (3.2) become different from zero. The Rayleigh (3.3) and high-frequency terms (3.4) in this case tend to zero and do not make a contribution to the residual displacement field. Let us prove this statement.

The residual displacements that occur in the elastic medium under the action of the source (1.1) are due to the fact that, with time, the reduced displacement potential tends not to zero but to a constant value [in this case, the source function $f(t) \to 1$]. Thus, the continuous source functions $f(t)$ [$t \in [0, \infty)$] that satisfy the conditions $f(0) = 0$ and $f(\infty) = 1$ lead to residual displacements.

As a source function in (1.1) we use one of the simplest functions of the above-mentioned class:

$$f(t) = \begin{cases} [\varepsilon(t) - \varepsilon(t - t_{\text{rise}})]t, & 0 \leqslant t \leqslant t_{\text{rise}}, \\ \varepsilon(t - t_{\text{rise}}), & t \gg t_{\text{rise}}. \end{cases}$$

Here t_{rise} is the rise time to the stationary value. If t_{rise} is used as the time scale, the function $f(t)$ takes the form

$$f(t) = \begin{cases} [\varepsilon(t) - \varepsilon(t-1)]t, & 0 \leqslant t \leqslant 1, \\ \varepsilon(t-1), & t \gg 1, \end{cases}$$

and its second derivative is $f''(t) = \delta(t) - \delta(t-1)$, where $\delta(t)$ is the Dirac function.

Substitution of $f''(t)$ into formulas (3.6) gives displacements in the form of the difference of two fundamental solutions. For example, for the vertical displacement component in the Rayleigh wave, we obtain

$$u_{zR}(r, 0, t) = \frac{abd}{\gamma\vartheta\theta}\left\{S_0(r, az_0, \gamma\vartheta t) - S_0[r, az_0, \gamma\vartheta(t-1)]\right\}, \tag{6.1}$$

where $S_0(r, az_0, \gamma\vartheta t) = B/R$, $B = ((R - X)/2)^{1/2}$, $R = (X^2 + Y^2)^{1/2}$, $X = r^2 + a^2 z_0^2 - \gamma^2\vartheta^2 t^2$, and $Y = 2az_0\gamma\vartheta t$.

Fixing the values of r and z_0 and passing to the limit $t \to \infty$, we have

$$R \to \gamma^2\vartheta^2 t^2, \quad R - X \to 2\gamma^2\vartheta^2 t^2, \quad \lim_{t\to\infty} S_0(r, az_0, \gamma\vartheta t) = 1/\gamma\vartheta t. \tag{6.2}$$

It follows from (6.1) and (6.2) that, as $t \to \infty$, the displacement u_{zR} tends to zero not more slowly than t^{-1}.

The proof for the horizontal displacement component in the Rayleigh wave and for the high-frequency displacement components (3.4) is derived in a similar manner.

As a result, we obtain the following values of the residual displacements in the half-space $z \geqslant 0$:

$$u_r^\infty(r,z) = \frac{r}{\rho_1^3} - \frac{r}{\rho_2^3}\left\{1 - \frac{2}{1-\gamma^2}\left[1 - 3(1-\gamma^2)\frac{z_2 z}{\rho_2^2} + 3\gamma^2(t_S^2 - t_P^2)\frac{4z_2^2 - r^2}{\rho_2^4}\right]\right\},$$
$$u_r^\infty(r,z) = -\frac{z_1}{\rho_1^2} - \frac{z_2}{\rho_2^2}\left\{1 - \frac{2}{1-\gamma^2}\left[\gamma^2 + (1-\gamma^2)\frac{(2z_2^2 - r^2)z}{\rho_2^2 z_2} - 3\gamma^2(t_S^2 - t_P^2)\frac{2z_2^2 - 3r^2}{\rho_2^4}\right]\right\}. \tag{6.3}$$

As can be seen from (6.3), the displacement of the ground proceeds toward the free surface (this is shown by the minus sign in the formula for the vertical displacement component). As a result, the initial horizontal free surface of the half space becomes dome-shaped after the explosion — a buckling hill forms.

The residual displacements of the free surface can be obtained from (6.3) for $z = 0$ or from (3.7) for $t \to \infty$. In dimensional variables, these displacements are

$$u_r^\infty = \Phi(\infty)\frac{2}{1-\gamma^2}\frac{r}{\rho^3}, \quad u_z^\infty = -\Phi(\infty)\frac{2}{1-\gamma^2}\frac{z_0}{\rho^3}, \quad \rho = (r^2 + z_0^2)^{1/2}. \tag{6.4}$$

We denote the abscissa and ordinate of points on the profile of the displaced free surface by x and y. Then, the parametric equation for the profile of the elastic buckling hill can be written as

$$x = r + \lambda\frac{r}{\rho^3}, \quad y = -\lambda\frac{z_0}{\rho^3}, \quad \lambda \equiv \frac{2}{1-\gamma^2}\Phi(\infty), \tag{6.5}$$

where the initial coordinate r of the point on the surface $z = 0$ acts as a parameter.

The surface of the hill is the surface of revolution of curve (6.5) around the y axis. Hence it follows that the volume of the hill can be found from the formulas

$$V_h = \pi\int_0^{y_m} x^2(r)\,dy = \pi\int_0^\infty (1 + \lambda/\rho^3)^2 r^2 y'(r)\,dr = 3\pi\lambda z_0\int_0^\infty (1 + 2\lambda/\rho^3 + \lambda^2/\rho^6)\,r^3\rho^{-5}dr$$
$$= 6\pi\lambda\left[\frac{1}{3} + \frac{\lambda}{12 z_0^3} + \frac{1}{63}\left(\frac{\lambda}{z_0^3}\right)^2\right] \qquad (y_m = \lambda/z_0^2). \tag{6.6}$$

We show that the inequality $\lambda z_0^{-3} \ll 1$ holds. Indeed, the smallest depth of explosion is about 50 m/kton$^{1/3}$. Otherwise, ejection of ground with the formation of a crater is inevitable [8]. The earth's soils are characterized by the value of $\Phi(\infty) \approx 10^3$ m^3/kton, and the largest value of the parameter is $\gamma^2 = 0.5$.

Hence, we obtain

$$\frac{\lambda}{z_0^3} = \frac{2}{1-\gamma^2}\frac{\Phi(\infty)}{z_0^3} \leqslant 4\frac{10^3 \text{ m}^3/\text{kton}}{125\cdot 10^3 \text{ m}^3/\text{kton}} = 0.03.$$

With an error less than a fraction of a percent, from (6.6) we have an approximate expression for the volume of the elastic buckling hill:

$$V_h = 2\pi\lambda = 4\pi\Phi(\infty)/(1-\gamma^2). \tag{6.7}$$

As can be seen from formula (6.7), the volume of the elastic buckling hill is a factor of $(1-\gamma^2)^{-1}$ larger than the volume displaced from the center of explosion. Hence it follows that the ground in the region of the hill for $\gamma \neq 0$ ($\gamma = 0$ corresponds to the liquid) is in the state of extension. The volume of the elastic buckling hill (6.7) is proportional to the explosion energy and is large for large-scale explosions.

If the elastic buckling hill is considered as an engineering building, its disadvantage is the small height. Indeed, the minimal depth of an explosion at which the explosion can be considered camouflet must be smaller than the elastic radius of the explosion, i.e., $z_0 \geqslant r_1$. For typical rocks, $r_1 \approx 100$ m/kton$^{1/3}$ [5]. For example, for stone salt, $r_1 = 95$ m/kton$^{1/3}$ [4].

From the second of Eqs. (6.4) we obtain the inequality

$$y_m = \max|u_z^\infty| = \max\left|\frac{2}{1-\gamma^2}\frac{\Phi(\infty)}{z_0^2}\right| \leqslant 4\,\frac{10^3\ \mathrm{m}^3/\mathrm{kton}}{(100\ \mathrm{m/kton}^{1/3})^2} = 0.4\ \mathrm{m/kton}^{1/3}.$$

Since the height of the hill increases in proportion to the cubic root of the explosion energy, one might have expected to obtain an arbitrarily high hill at sufficiently large explosion energy. However, the factor that restricts the height of the hill is the gravity force.

With increase in the explosion energy, the dimension of the camouflet cavity increases and the stability of the vault of the cavity decreases. For certain dimensions of the cavity, the ground caves in and caving gradually propagates to the free surface. As a result, a crater occurs in the vicinity of the top of the buckling hill. The edges of the crater are formed by the peripheral parts of the buckling hill, which have insignificant height.

The formation mechanism of the buckling hill presented in this paper predominates for large depth of explosion at which the ground at the zero point is elastically deformed.

For comparatively small depths of explosion, which are used in blasting to loosen ground, the predominant mechanism of formation of a buckling hill is different. In this case, most of the hill is formed by the loosening of the ground due to rupture, dispersion, and the return fall into the crater.

REFERENCES

1. K. I. Ogurtsov and G. I. Pterashen', "Dynamic problems for an elastic half-space in the case of axial symmetry," *Uch. Zap. Leningrad Univ.*, No. 149, Issue 24, 3–117 (1951).
2. N. I. Onis'ko and E. I. Shemyakin, "Motion of the free surface of homogenous ground in an underground explosion," *Prikl. Mekh. Tekh. Fiz.*, No. 4, 82–93 (1961).
3. A. S. Tyapin and A. I. Startsev, "Compact representation of the fundamental solution of the internal Lamb problem on the free surface," *Prikl. Mekh. Tekh. Fiz.*, No. 1, 126–132 (1992).
4. J. H. Healy, King Chi-Yu, and O'Neill, "Source parameters of the Salmon and Starling nuclear explosions from seismic measurements," *J. Geophys. Res.*, **76**, No. 14, 3344–3335 (1971).
5. N. A. Haskell, "Analytic approximation for the elastic radiation from a contained underground explosion," *J. Geophys. Res.*, **76**, No. 10, 2583–2587 (1967).
6. Aki Keiti, M. Bouchon, and P. Reasenberg, "Seismic source function for an underground nuclear explosion," *Bull. Seismol. Soc. Am.*, **64**, No. 1, 131–148 (1974).
7. J. A. Sharpe, "The production of elastic waves by explosion pressure," *Geophysics*, **7**, No. 2, 144–154 (1942).
8. M. A. Sadovskii (ed.), *Mechanical Effect of an Underground Explosion* [in Russian], Nedra, Moscow (1971).
9. R. A. Mueller and J. R. Murphy, "Seismic characteristics of under-ground nuclear detonations. Pt 1. Seismic spectrum scaling," *Bull. Seismol Soc. Am.*, **61**, No. 6, 1675–1692 (1971).
10. H. C. Roden, "Inelastic processes in seismic waves generation by underground explosions," in: E. S. Hysebye and Mykkeltveit (eds.) *Identification of Seismic Sources — Earthquake or Underground Explosion*, Reidel Publ., Dordrecht–Boston–London (1981).
11. M. A. Lavrent'ev and B. V. Shabat, *Methods of the Theory of Functions of a Complex Variable* [in Russian], Fizmatgiz, Moscow (1951).
12. G. Werth and P. Randolph, "The Salmon seismic experiment," *J. Geophys. Res.*, **71**, No. 14, 3406–3413 (1966).
13. D. W. Patterson, "Nuclear decoupling, full and partial," *ibid.*, pp. 3427–3436.
14. L. A. Rogers, "Free-field motion near a nuclear explosion in salt: project Salmon," *ibid.*, pp. 3415–3426.
15. *Peaceful Nuclear Explosion*, Proc. Panel Vienna, 2–4 March, 1970, IAEA, Vienna (1970).
16. D. Rawson, P. Randolph, C. Bourdman, and V. Wheeler, "Post-explosion environment resulting from the Salmon event," *J. Geophys. Res.*, **71**, No. 14, 3507–3521 (1966).